Available online at www.sciencedirect.com
SCIENCE DIRECT®
Nuclear Engineering and Design 235 (2005) 1239–1249
Nuclear Engineering and Design
www.elsevier.com/locate/nucengdes

Statistics of velocity and preferential accumulation of micro-particles in boundary layer turbulence

Maurizio Picciotto[a], Cristian Marchioli[a], Michael W. Reeks[b], Alfredo Soldati[b,*]

[a] *Centro Interdipartimentale di Fluidodinamica e Idraulica and Dipartimento di Energetica e Macchine, University of Udine, v.le delle Scienze 208, 33100 Udine, Italy*

[b] *School of Mechanical and Systems Engineering, University of Newcastle upon Tyne, Newcastle upon Tyne NE1 7RU, UK*

Received 13 January 2005; received in revised form 14 January 2005; accepted 25 January 2005

Abstract

The distribution of inertial particles in turbulent flows is strongly non-homogeneous and is driven by the structure of the underlying carrier flow field. In this work, we use DNS combined with Lagrangian particle tracking to characterize the effect of inertia on particle preferential accumulation. We compare the Eulerian statistics computed for fluid and particles of different size, and observe differences in terms of distribution patterns and deposition rates which depend on particle inertia. Specifically, different statistics are related to the selective interaction occurring between particles and coherent flow structures. This selective response causes a preferential sampling of the flow field by the particles and eventually leads to the well-known phenomenon of long-term particle accumulation in the boundary layer. We try to measure particle preferential accumulation with a Lagrangian parameter related to the rate of deformation of an elemental volume of the particle phase along a particle trajectory. In the frame of the Lagrangian approach, this parameter is mathematically defined as the particle position Jacobian, $J(t)$, computed along a particle path. This quantity is related to the local compressibility/divergence of the particle velocity field. Lagrangian statistics of $J(t)$ show that compressibility increases for increasing particle response times τ_p^+ (up to $\tau_p^+ = 25$ and within the time span covered by the simulation).

1. Introduction

In a number of environmental and industrial problems involving turbulent dispersed flows, the information on particle distribution is a crucial issue. In this respect, time-averaged volume-averaged concentrations based on point closure models are not sufficient and more sophisticated models are required.

Turbulent flow fields are characterized by a strongly organized and coherent nature represented by large scale structures. These structures, because of their coherence and persistence have a significant influence on the transport of dispersed particles. Specifically, coherent flow structures generate preferentially directed, non-random motion of particles leading to non-uniform concentration and to long-term accumulation.

* Corresponding author.
E-mail address: soldati@uniud.it (A. Soldati).

0029-5493/$ – see front matter © 2005 Elsevier B.V. All rights reserved.
doi:10.1016/j.nucengdes.2005.01.013

Preferential accumulation of particles by coherent structures has been examined previously in a number of theoretical and experimental works (Caporaloni et al., 1975; Reeks, 1977, 1983; Maxey, 1987; Wang and Maxey, 1993; Eaton and Fessler, 1994). In the case of homogeneous turbulence (Reeks, 1977; Maxey, 1987; Wang and Maxey, 1993; Eaton and Fessler, 1994), the particle concentration field will be characterized by local particle accumulation in regions of low vorticity and high strain. In the case of non-homogeneous turbulence (Caporaloni et al., 1975; Reeks, 1977), as for instance the turbulent boundary layer, the local interaction between particles and turbulence structures will lead to a remarkably macroscopic behavior producing particle accumulation in the viscous sublayer (Marchioli and Soldati, 2002; Marchioli et al., 2003; Narayanan et al., 2003). This effect may be of fundamental significance in applications as particle abatement, flow reactors and control of momentum, heat and mass fluxes at a wall.

Several attempts have been made to characterize the regions of particle preferential accumulation. In particular, Rouson and Eaton (2001) used the topological classification by Chong et al. (1990) and observed that, very near the wall, strong vortical regions are depleted of particles, which accumulate in specific convergence regions. Rouson and Eaton (2001) have also shown that, farther away from the wall, the spatial intermittency of particle distribution is not correlated with the topological descriptors even if particle concentration remains highly non-uniform suggesting that the characterization of particle clustering and the link with turbulent structure requires deeper analyses.

In a previous work (Marchioli and Soldati, 2002), we analyzed the mechanisms leading to particle accumulation with specific focus on the interactions of particles with the local turbulent structure, describing an instantaneous phenomenological picture. In the first part of the present work, we examine the influence of inertia on particle preferential sampling of a turbulent channel flow. Specifically, we aim at providing a statistical characterization of particle velocity to analyze the selective response of inertial micro-particles to the structure of the underlying turbulent flow field. The second part of this work focuses on particle segregation in clusters, a well-known macroscopic phenomenon produced by particle response to coherent structures. Particle clustering suggests that the dispersed phase, when considered as a continuum, can be characterized by high levels of compressibility in spite of the incompressibility of the carrier flow field. Our object is precisely to characterize the compressibility of the "particle phase" by means of a single Lagrangian parameter. In the frame of the Lagrangian approach, we use the Jacobian of particle path evaluated along the trajectory of each single particle (Osiptsov, 1998). The Jacobian can be related to the rate of deformation of an elemental volume of particles moving along the given particle trajectory. Specifically, the time derivative of the Jacobian corresponds to the local divergence or local compressibility of the instantaneous particle velocity field (Aris, 1989; Pope, 2000).

2. Methodology

2.1. DNS of turbulent channel flow

The flow into which particles are introduced is a turbulent Poiseuille channel flow of air, assumed incompressible and Newtonian. The reference geometry consists of two infinite flat parallel walls: the origin of the coordinate system is located at the center of the channel and the x-, y- and z-axes point in the streamwise, spanwise and wall-normal directions, respectively. Periodic boundary conditions are imposed on the fluid velocity field in both streamwise and spanwise directions, no-slip boundary conditions are imposed at the walls. All variables are normalized by the wall friction velocity u_τ, the fluid kinematic viscosity ν and the half channel height h. The friction velocity u_τ is defined as $u_\tau = (\tau_w/\rho)^{1/2}$, where τ_w is the mean shear stress at the wall and ρ is the fluid density. Thus, the balance equations in dimensionless form are:

$$\frac{\partial u_i}{\partial x_i} = 0, \tag{1}$$

$$\frac{\partial u_i}{\partial t} = -u_j \frac{\partial u_i}{\partial x_j} + \frac{1}{Re} \frac{\partial^2 u_i}{\partial {x_j}^2} - \frac{\partial p}{\partial x_i} + \delta_{1,i}, \tag{2}$$

where u_i is the ith component of the dimensionless velocity vector, p is the fluctuating kinematic pressure, $\delta_{1,i}$ is the mean dimensionless pressure gradient that drives the flow and $Re_\tau = u_\tau h/\nu$ is the shear Reynolds number. Eqs. (1) and (2) are solved using a pseudo-spectral method. Details of the numerical method can be found elsewhere (Lam and Banerjee, 1992).

In the present study, we consider air with density $\rho = 1.3\,\mathrm{kg\,m^{-3}}$ and kinematic viscosity $\nu = 15.7 \times 10^{-6}\,\mathrm{m^2\,s^{-1}}$. The calculations are performed on a computational domain of $1885 \times 942 \times 300$ wall units in x, y and z discretized with $128 \times 128 \times 129$ nodes. The shear Reynolds number is $Re_\tau = 150$ and the time step used is $\Delta t^+ = 0.045$ in wall time units. The statistics of the flow field are consistent with previous simulations (Kim et al., 1987; Lyons et al., 1991).

2.2. Lagrangian particle tracking

Particles are injected into the flow at concentration low enough to consider dilute system conditions (particle–particle interactions are neglected). Furthermore, particles are assumed to be pointwise, rigid and spherical. The motion of particles is described by a set of ordinary differential equations for particle velocity and position at each time step. For particles much heavier than the fluid ($\rho_\mathrm{p}/\rho \gg 1$, ρ_p particle density), Elghobashi and Truesdell (1992) have shown that the only significant forces are Stokes drag and buoyancy and that Basset force can be neglected being an order of magnitude smaller. In the present work, the effect of gravity has also been neglected. With the above simplifications the following Lagrangian equation for the particle velocity is obtained (Maxey and Riley, 1983):

$$\frac{\mathrm{d}\mathbf{u}_\mathrm{p}}{\mathrm{d}t} = -\frac{3}{4}\frac{C_\mathrm{D}}{d_\mathrm{p}}\left(\frac{\rho}{\rho_\mathrm{p}}\right)|\mathbf{u}_\mathrm{p} - \mathbf{u}|(\mathbf{u}_\mathrm{p} - \mathbf{u}), \tag{3}$$

where $\mathbf{u}_\mathrm{p}$ and $\mathbf{u}$ are the particle and fluid velocity vectors, d_p is the particle diameter and C_D is the drag coefficient given by:

$$C_\mathrm{D} = \frac{24}{Re_\mathrm{p}}(1 + 0.15\,Re_\mathrm{p}^{0.687}), \tag{4}$$

where Re_p is the particle Reynolds number ($Re_\mathrm{p} = d_\mathrm{p}|\mathbf{u}_\mathrm{p} - \mathbf{u}|/\nu$). The correction for C_D is necessary because Re_p does not necessarily remain small (Crowe et al., 1998), in particular for depositing particles.

A Lagrangian particle tracking code coupled with the DNS code was developed to calculate particles paths in the flow field. The code interpolates fluid velocities at discrete grid nodes onto the particle position, and with this velocity the equations of motion of the particle are integrated with time.

The interpolation scheme exploits a sixth order Lagrangian polynomials. A fourth-order Runge–Kutta scheme is implemented for time integration. The interpolation scheme used was compared both with spectral direct summation and with an hybrid scheme which exploits sixth order Lagrangian polynomials in the streamwise and spanwise directions and Chebychev summation in the wall-normal direction: results showed good agreement between the three schemes. For the simulations presented here, four sets of 10^5 particles were considered, characterized by different relaxation times, defined as $\tau_\mathrm{p} = \rho_\mathrm{p} d_\mathrm{p}^2/18\mu$, where μ is the fluid dynamic viscosity. τ_p is made dimensionless using wall variables and the Stokes number is obtained. In the present paper we have $\tau_\mathrm{p}^+ = St = 0.2, 1, 5$ and 25.

At the beginning of the simulation, particles are distributed homogeneously over the computational domain and their initial velocity is set equal to that of the fluid in the particle initial position. Periodic boundary conditions are imposed on particles in both streamwise and spanwise directions, elastic reflection is applied when the particle center is less than a distance $d_\mathrm{p}/2$ from the wall. Elastic reflection was chosen since it is the most conservative assumption when studying the reasons of particle prefential concentration in a turbulent boundary layer. We will not analyze the effect of the elastic reflection boundary condition on particle behavior, since it is beyond the scope of this paper. In this work we are more interested in the influence of turbulence on particle behavior than vice versa. We thus employ the "one-way coupling" approximation under which particles do not feedback on the flow field.

3. Results

3.1. Effect of inertia on particle preferential accumulation

Interactions between particles and the turbulent field are influenced by particle relaxation time. In this section, we analyze this influence from a statistical viewpoint. Specifically, we compare the Eulerian statistics of the fluid velocity field with those of the particle velocity field and with those of the fluid velocity field sampled by particles.

Fig. 1 shows the mean streamwise velocity profile (averaged in time and along the *xy* planes) for both particles and fluid as a function of the wall-normal coordinate z^+. Profiles are averaged over the last 500 time instants of the simulation. Differences are readily visible, but there is evidence of an effect of particle inertia. Smaller particles ($\tau_p^+ = 0.2$) behave like fluid tracers and their mean velocity profile (dotted line) matches almost perfectly that of the fluid (open circles). As particle relaxation time increases, the mean particle velocity is seen to lag the mean fluid velocity outside the viscous sublayer, in the region $5 < z^+ < 50$. The most important differences are observed for the larger particles ($\tau_p^+ = 5$ and $\tau_p^+ = 25$) approximately in the region $10 < z^+ < 30$. Similar results were reported also by van Haarlem et al. (1998), Portela et al. (2002) and Narayanan et al. (2003). As already observed by van Haarlem et al. (1998), this behavior is probably due to the fact that inertial particles dispersed in a turbulent flow do not sample the flow field homogeneously. Once in the near wall region, particles tend to avoid areas of high vorticity preferring areas characterized by lower-than-mean streamwise fluid velocity and by high strain rate. This effect is confirmed by statistics of the root mean square (RMS) of velocity fluctuations for both phases, shown in Fig. 2. Fig. 2(a) compares the RMS of particle streamwise velocity with that of the fluid, as function of z^+. Fluctuations of particle streamwise velocity are larger than those of the fluid and this difference becomes more evident as particle relaxation time increases. The RMS profiles of the fluid velocities at the position of the particles (not shown) closely follow the behavior of particle RMS profiles. Similar results for the streamwise velocity fluctuations were reported by Portela et al. (2002) for particles in pipe flow.

From a physical viewpoint, the difference in the streamwise values suggests that the gradient in the mean velocity of the fluid can produce significant fluctuations of the streamwise particle velocity. Due to their interaction with near-wall coherent structures, particles move across the channel and perpendicularly to the mean flow, between regions of high and low streamwise-velocity (Portela et al., 2002). This seems particularly true in the case of heavy particles, with a large Stokes number and a long "memory". As a consequence, particles with streamwise velocities very different from each other can be found confined in the same fluid environment. This is not true for fluid particles, which show no preferential concentration: the local instantaneous streamwise velocity is more homogeneous and the corresponding fluctuation is smaller than that of the particle velocity field. As reported by Portela et al. (2002) "The gradient in the mean-streamwise velocity is potentially much more important when there exists a net flow of particle toward the wall, as it is in the case with absorbing walls, or not fully developed flows". This is a characteristic feature of particles dispersed in shear flows (Reeks, 1993).

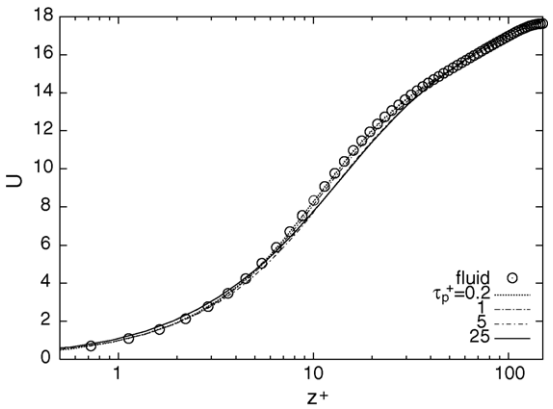

Fig. 1. Mean streamwise velocity profiles for the particles (lines) and the fluid (symbol).

An opposite behavior is observed in the spanwise direction and in the wall-normal direction (Fig. 2(b) and (c), respectively), where the fluid velocity field has zero mean gradient. The turbulence intensity of the particle-phase is lower than that of the fluid due to two mechanisms acting in tandem. The first mechanism is preferential concentration of particles in low-speed regions, characterized by lower turbulence intensity. The second is the filtering of high frequency or wavenumber fluctuations done by particles due to their inertia The inertial filtering damps turbulence intensity of the particle field in the wall-normal direction and in the spanwise direction. Similar filtering effect has been observed in homogeneous turbulence (Reeks, 1993).

Note that preferential concentration is related to pattern formation of particle clusters whereas inertial filtering refers to the incomplete response of a single particle to its fluctuating fluid environment. A further difference is that preferential concentration depends on particle inertia in a rather complex way whereas the inertial filtering effect increases monotonically

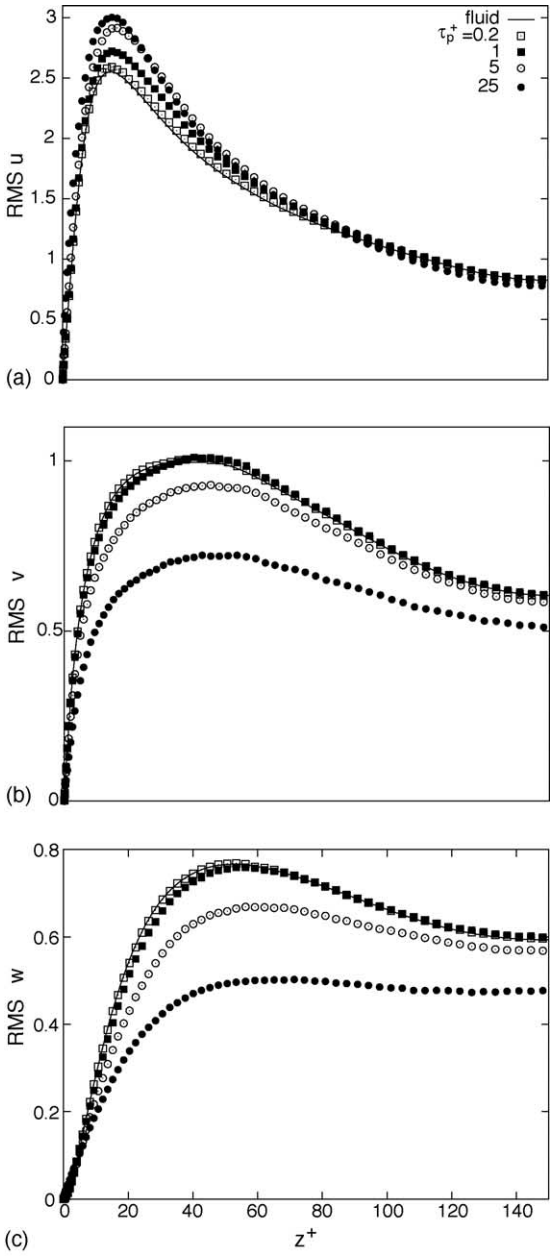

Fig. 2. Root mean square of the velocity fluctuations for particles (symbols) and fluid (drawn line): streamwise (a); spanwise (b); wall-normal (c).

with particle inertia (Narayanan et al., 2003). Smaller particles ($\tau_p^+ = 0.2$ and $\tau_p^+ = 1$) are more sensitive to the fluid velocity fluctuations: their spanwise and wall-normal RMS profiles are very close to those of

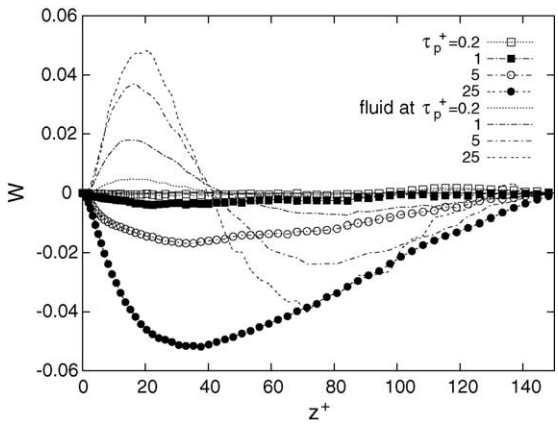

Fig. 3. Mean wall-normal velocity; particles, and fluid at particle position.

the fluid. Larger particles ($\tau_p^+ = 5$ and $\tau_p^+ = 25$) are less sensitive and their velocity fluctuations are smaller than those of the fluid (Brooke et al., 1992). The inertial filtering in the wall-normal direction will cause a drift leading to a net wallward velocity of the particle-phase (Brooke et al., 1992; Narayanan et al., 2003). This drift velocity is influenced by inertia (Brooke et al., 1992) and may have significant implications in a number of technological and environmental applications since it also determines the non-uniform particle distribution in the wall-normal direction.

In Fig. 3 we show the time-averaged (500 instants) wall-normal velocity profiles for the different particle sets, plotted against the fluid wall-normal velocity *at particle position*. Recall that the wall-normal velocity is directed toward the wall if negative and away from the wall if positive. Particle velocity profiles (symbols) drop to zero at the wall ($z^+ = 0$) and at the channel centerline ($z^+ = 150$), whereas their modulus is maximum in the region $20 < z^+ < 40$ roughly. This maximum value increases as particle inertia increases: a difference of more than one order of magnitude is observed between the maximum velocities of $\tau_p^+ = 0.2$ and $\tau_p^+ = 25$ particles. Our results confirm that, up to $\tau_p^+ = 25$, an increase in the inertia will correspond to an increase in the wall-normal turbophoretic accumulation.

Now consider the fluid velocity at particle position (Fig. 3, lines). We can observe a behavior which is monotonic with particle inertia: the fluid wall-normal

velocities at particle position are different from zero on average and their maxima and minima increase with particle inertia. In the near-wall region ($0 < z^+ < 40$), the fluid wall-normal velocity at particle position is positive (i.e. directed away from the wall) reaching a local maximum at $z^+ = 20$ roughly: particles in this region sample preferentially ejection-like environments. The fluid wall-normal velocity at particle position becomes negative (i.e. directed toward the wall) outside the near wall region reaching a local maximum at 70–80 z^+.

The sampling of regions with positive wall-normal fluid velocity done by particles can be interpreted as a sort of continuity effect of the fluid velocity field for which sweep events, characterized by negative wall normal fluid velocity (directed toward the wall), are more intense and spatially concentrated than ejection events, characterized by positive wall-normal fluid velocity (directed away from the wall).

To examine in further detail the profiles shown in Fig. 3, in Fig. 4 we plotted vis-á-vis the particle wall-normal velocity against the fluid wall-normal velocity computed at particle position. We show the comparison for each particle set, using an appropriate scaling for the velocity axis.

Far away from the wall, small inertia particles are expected to follow promptly the fluid: indeed, the velocity profile of $\tau_p^+ = 0.2$ particles (line with empty squares in Fig. 4(a)) is similar to that of the fluid (line with black squares in Fig. 4(a)) in the region $100 < z^+ < 150$. Approaching the wall region ($z^+ < 100$), particles seem to lag the fluid. In particular, particle wall-normal velocity (though small) remains negative whereas the wall-normal velocity of the fluid at the position of $\tau_p^+ = 0.2$ particles reaches a local negative peak at $z^+ \approx 80$, then becomes positive in the near wall region ($z^+ < 50$) with a further local peak at $z^+ \approx 20$.

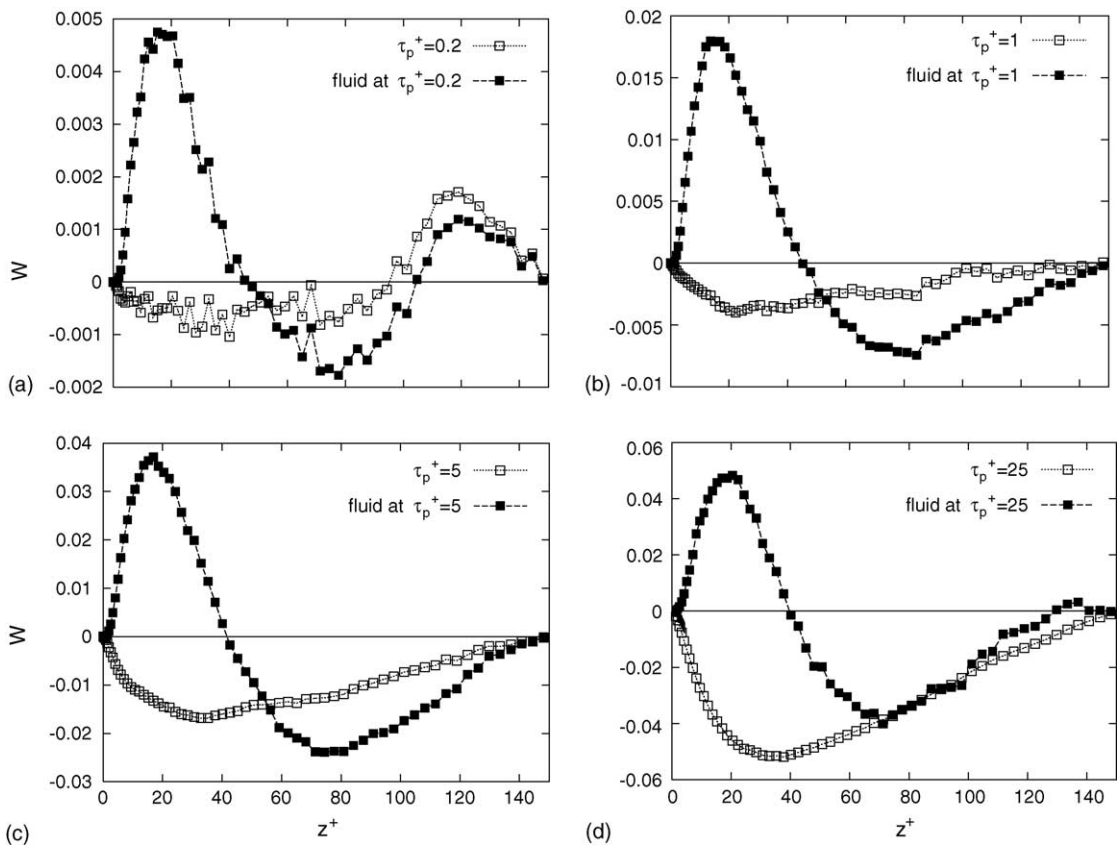

Fig. 4. Mean wall-normal velocities; (a)–(d), comparison for each particle set between particle and fluid at particle position wall-normal velocity.

When particle inertia increases (Fig. 4(b)–(d)), our results indicate more clearly that particles have a wall-normal velocity directed toward the wall, on average. The velocity profiles for $\tau_p^+ = 1$ and $\tau_p^+ = 5$ (Fig. 4(b) and (c), lines with empty boxes) are similar, though different in magnitude: for $50 < z^+ < 150$, these particles sample regions where the fluid wall-normal velocity is larger than that of the particles and is directed toward the wall. In the near-wall region ($z^+ < 50$), the fluid velocity becomes positive whereas the particle wall-normal velocity reaches a peak approximately equal to -0.004 and -0.015 for $\tau_p^+ = 1$ particles (Fig. 4(b)) and for $\tau_p^+ = 5$ particles (Fig. 4(c)), respectively. Profiles for $\tau_p^+ = 25$ particles (Fig. 4(d)) scale in a similar way with respect to $\tau_p^+ = 1$ and $\tau_p^+ = 5$ particles, except in the region $50 < z^+ < 150$, where their wallward velocity becomes comparable or slightly larger than that of the underlying flow field. The above results confirm that (i) particles undergo a wallward drift which increases with particle inertia and that (ii) particles approaching the wall ($z^+ < 50$) sample preferentially flow regions where the fluid has wall-normal velocity directed toward the outer layer. To explain how, on average, particles can travel toward the wall in spite of an environment of adverse flow, let us recall the interaction between particles and sweep events. Particles are trapped by the sweeps in the outer region, where they find a "favorable" fluid velocity field (on average) and gain sufficient momentum to approach the wall (turbophoretic drift). Around the cross-over point of the averaged wall-normal fluid velocity (located at $z^+ = 40$–45 roughly, in Figs. 3 and 4), particles moving toward the wall start feeling an "adverse" velocity field which acts to damp their turbophoretic drift. As a result, particle wall-normal velocity (profiles with symbols in Fig. 3) starts decreasing after the cross-over. Again, this decrease is more evident for particles with larger Stokes number and a "longer" memory, the averaged wall-normal velocity of the smaller particles being much smaller in magnitude.

The statistics provided in previous figures pinpoint the important role played by the inertial sampling in determining the intensity of particle preferential fluxes toward the wall which in turn are responsible for long-term particle accumulation in the near wall region. In Fig. 5, we plot the instantaneous space average particle concentration (taken at time $t^+ = 1125$) for all particle sets. The concentration represents particle number density and was calculated by dividing the channel into wall-parallel bins following the Chebychev collocation method: for each bin we counted the number of particles, normalized by the total number of particles and then multiplied by a proper shape factor to account for the non-uniform spacing of the bins. A log–log scale is used to capture the different behavior of the profiles in the proximity of the wall and to underline the different magnitude of particle concentration for each relaxation time. Modifications in the particle concentration profiles are rather different for each particle set. $\tau_p^+ = 0.2$ Particles with $\tau_p^+ = 0.2$ seem to be weakly involved in the accumulation process. As the particle relaxation time increases, the accumulation process takes up more quickly. Concentration profiles for the $\tau_p^+ = 1$ and the $\tau_p^+ = 5$ particles reach a peak value near $z^+ = 1$ which is about one and two orders of magnitude higher than that observed for the smaller particles, respectively. The concentration profile for the $\tau_p^+ = 25$ particles develops a sharp peak well into the viscous sublayer at $z^+ \approx 0.4$–0.5: at time $t^+ = 1125$ the normalized particle concentration in this region is $O(10^2)$ times larger than the initial value. Recall that the dimensionless value of particle diameter d_p^+ are: 0.0648, 0.153, 0.342 and 0.765 for $\tau_p^+ = 0.2$, 1, 5 and 25, respectively. The tendency of particle accumulation to increase with the relaxation time has been already observed (Brooke et al., 1992; van Haarlem et al., 1998) and is correlated with the different intensity of particle wall-normal velocities observed in Figs. 3 and 4.

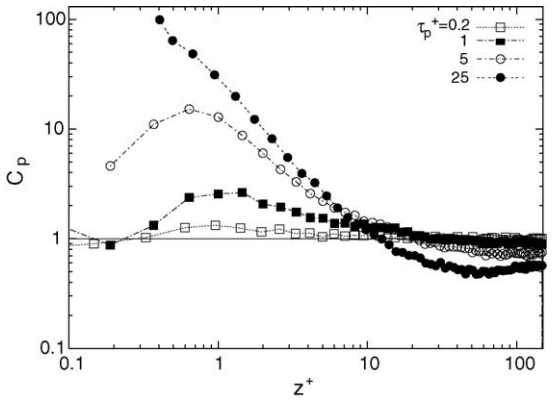

Fig. 5. Mean particle concentration profiles as function of the wall-normal coordinate (z^+) for all particle sets at time $t^+ = 1125$.

We remark here that the process of particle accumulation has not reached a steady state within the time span covered by the simulation ($t^+ = 1190$): the peak values of particle concentration in the near wall region are still increasing with time and the process shows no tendency toward saturation, as might be expected at later stages of the simulation (Portela et al., 2002).

3.2. Characterization of local particle segregation

The Eulerian statistics reported in the previous section provide useful quantitative information about particle preferential sampling of specific flow regions. This preferential sampling causes particle drift toward the wall and determines their local accumulation. Particles form clusters so that their ensemble behaves like a compressible fluid. Here, we are interested in quantifying the local concentration of particle ensembles characterized by different relaxation times. This can be done straightforwardly by counting particles in an Eulerian grid, a procedure which is very expensive from a computational viewpoint. Another possibility can be the calculation of the divergence of particle velocity field, from which the time evolution of the concentration field would be available. However, in the frame of the Eulerian–Lagrangian approach the dispersed phase may not be treated like a real compressible fluid with a differentiable velocity field. Thus, Eulerian equations for the dispersed phase cannot be derived and compressibility cannot be evaluated by calculating the deformation rate. To circumvent this problem, we calculate the Jacobian $J(t)$ of particle path, evaluated along the trajectory of each single particle. Then, we will relate the value of the Jacobian to particle accumulation with respect to the underlying flow structure. This methodology is based on the idea that the motion of each particle can be described by a point transformation (Aris, 1989). Let us consider the time $t = 0$ as the first instant in which particles are injected into the domain. Be $\mathbf{X}_0$ the initial position of a given particle: at a later time t, the same particle will be at position $\mathbf{X}$. Without loss of generality, we can say that $\mathbf{X}$ is a function of t and $\mathbf{X}_0$:

$$\mathbf{X} = \mathbf{X}(\mathbf{X}_0, t). \tag{5}$$

Then we consider an elemental volume $\mathrm{d}V_0$ surrounding the particle (i.e. continuum approach) with the aim of following its evolution along the particle path. The elemental volume $\mathrm{d}V_0$ is about the point $\mathbf{X}_0$ at time $t = 0$. Then the volume is moved and distorted but does not break up because the motion is continuous: at time t, the volume is about the point $\mathbf{X}$. If the coordinate system is changed from coordinates $\mathbf{X}_0$ to coordinates $\mathbf{X}$, the elemental volume is $\mathrm{d}V = J(t)\,\mathrm{d}V_0$, where J is the Jacobian of the particle path. The Jacobian $J(t)$ is equal to $\det[\partial X_i(\mathbf{X}_0, t)/X_{0j}]$ and quantifies the dilatation/compression of the initial volume. Thus, $J(t)$ represents a mapping of particle field – instantaneously sampled for a specific particle path – with respect to a given initial condition in which we suppose uniform particle elements, namely $J(t = 0) = 1$. Note that $J(t)$ can be related to the divergence of the particle velocity field, which also quantifies the local compressibility of the particle velocity field, through the following equation (Aris, 1989; Pope, 2000):

$$\frac{\mathrm{d}\ln|J(t)|}{\mathrm{d}t} = \nabla \cdot \mathbf{u}_\mathrm{p}. \tag{6}$$

We have an important physical meaning for the divergence of the particle velocity field: it represents the relative rate of change of the dilatation/compression following a particle path (Aris, 1989). Our objective here is to use $J(t)$ to characterize the effect of inertia on the local compressibility of the particle velocity field. This quantity can be a measure of particle accumulation since it influences the drift toward the wall in the same way that it influences the settling velocity in homogeneous isotropic turbulence (Maxey, 1987) except that in this case the drift is driven by the inhomogeneity in the near wall turbulence and not by gravity.

To compute $J(t)$, we refer to Osiptsov's method (Osiptsov, 1998). Osiptsov's method is a full Lagrangian method for calculating the particle concentration and the particle velocity field in dilute gas-particle flows. This method (i) is based on integrating equations for the particle concentration along individual particle path, (ii) has great potential for dramatic reductions in computational time compared with the standard Eulerian–Lagrangian approach, (iii) can deal with steady and unsteady flows without change of algorithm, and (iv) the mathematical formulation provides a sound framework for interpreting the physics of the particle behavior: specifically, the method can handle certain types of singularities where the particle concentration becomes infinite, in a mathematical

sense. In Osiptsov's method, $J(t)$ is computed by integration along particle path and particle concentration is then obtained algebraically from the Lagrangian form of the particle continuity equation by computing the change in volume of an element of 'particle fluid' along its trajectory.

In Lagrangian form the conservation equations of mass and momentum for a particle element read:

$$C_{\mathrm{p}} = \frac{C_{0\mathrm{p}}}{|J(t)|}, \tag{7}$$

$$\frac{\mathrm{d}\mathbf{u}_{\mathrm{p}}}{\mathrm{d}t} = \frac{\mathbf{u} - \mathbf{u}_{\mathrm{p}}}{\tau_{\mathrm{p}}} \tag{8}$$

neglecting the effect of particle Reynolds number. $C_{0\mathrm{p}}$ is the initial particle phase concentration. C_{p}, $\mathbf{u}$ and $\mathbf{u}_{\mathrm{p}}$ are functions of two Lagrangian independent variables: the time, t, and the initial position, $\mathbf{X}_0$.

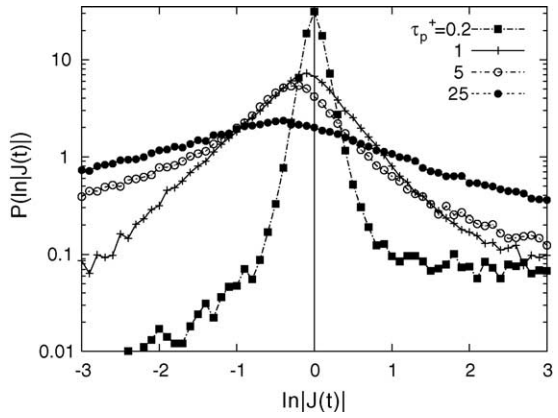

Fig. 6. PDF of particles as function of the Jacobian $J(t)$ at time $t^+ = 1125$.

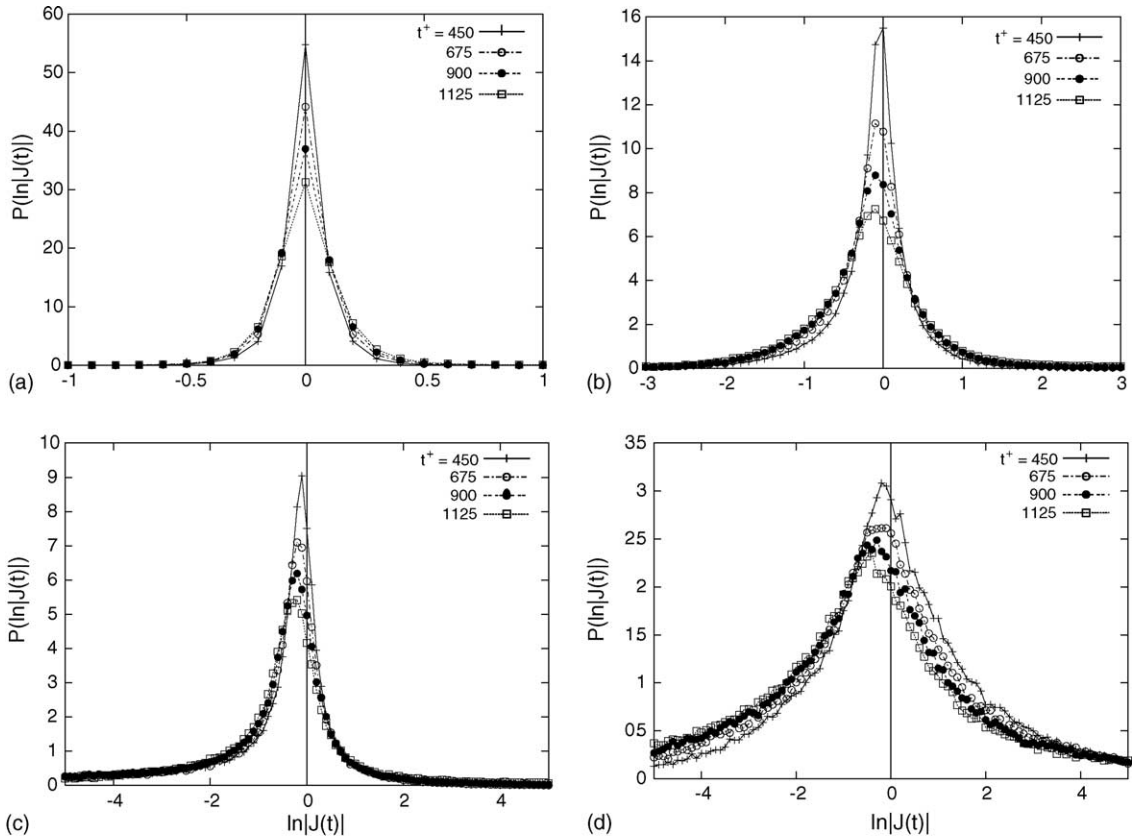

Fig. 7. PDF of particles as function of the $\ln|J(t)|$ for different times for particles with $\tau_{\mathrm{p}}^{+} = 0.2$ (a), 1 (b), 5 (c) and 25 (d).

Referring to the Osiptsov method (Osiptsov, 1998) and recalling that $d\mathbf{X}/dt = \mathbf{u}_p$, we can take the derivative of Eq. (8) and write:

$$\frac{d}{dt}\frac{\partial u_{pi}(\mathbf{X}_0,t)}{\partial X_{0j}} = \frac{1}{\tau_p}\left[\frac{\partial u_i(\mathbf{X},t)}{\partial X_k(\mathbf{X}_0,t)}\frac{\partial X_k(\mathbf{X}_0,t)}{\partial X_{0j}} - \frac{\partial u_{pi}(\mathbf{X}_0,t)}{\partial X_{0j}}\right], \quad (9)$$

$$\frac{d}{dt}\frac{\partial X_i(\mathbf{X}_0,t)}{\partial X_{0j}} = \frac{\partial u_{pi}(\mathbf{X}_0,t)}{\partial X_{0j}}. \quad (10)$$

Applying the initial conditions:

$$\frac{\partial X_i(\mathbf{X}_0,t=0)}{\partial X_{0j}} = \delta_{ij}, \quad (11)$$

$$\frac{\partial u_{pi}(\mathbf{X}_0,t=0)}{\partial X_{0j}} = \frac{\partial u_i(\mathbf{X}_0,t=0)}{\partial X_j}. \quad (12)$$

Eqs. (9) and (10) can be integrated numerically, along each particle pathline. Once the unknowns $\partial X_i/\partial X_{0j}$ are calculated, $J(t)$ can be computed.

The methodology described above can be used to calculate the evolution of a small elemental volume filled with a fixed number of particles along a specific pathline. Since particle movements are not necessarily correlated with the underlying carrier fluid motions, the small volume will undergo compression or expansion. A compression implies an increase of the local particle number density: particles belonging to the same elemental volume get even closer and a local accumulation takes place. On the other hand, expansion implies a growing volume i.e. a larger distance between particles belonging to the same elemental volume. To quantify the prevalence of these two competing effects, we calculated the statistics of $\ln|J(t)|$. Fig. 6 shows the PDF of particles as function of $\ln|J(t)|$ at time $t^+ = 1125$. For the smaller particles ($\tau_p^+ = 0.2$) the PDF is narrow, roughly centered around zero and skewed toward the $\ln|J(t)| > 0$ side. As the particle relaxation time increases, the PDF has a larger spreading and appears skewed toward the $\ln|J(t)| < 0$ side. Thus, larger particles preferentially sample flow regions where $J(t) < 1$. Following Eq. (7), we can conclude that the local particle concentration C_p in such convergence regions is higher than the initial value C_{0p}. Also, we observe that C_p is more focused for larger particles: Fig. 6 shows that sampled regions are characterized by values of $J(t)$ which become smaller as particle inertia increases.

In Fig. 7 the time evolution of the PDFs is plotted as function of $\ln|J(t)|$. This figure confirms that the tendency of particles to cluster and converge in specific flow regions is dominated by inertia. The PDF of $\tau_p^+ = 0.2$ particles (Fig. 7(a)) remains centered around the initial value of $J(t)$, showing that expansions and compressions of the dispersed phase are weak. Conversely, profiles for the larger particles shift toward smaller values of $J(t)$ continuously during the simulation. This is particularly evident for the $\tau_p^+ = 25$ particles (Fig. 7(d)). Recalling Eq. (6), a decrease of $J(t)$ in time implies that large inertia particle local velocity is preferentially "compressing", even if the underlying flow field is incompressible.

4. Concluding remarks

This paper addresses the issue of particle preferential concentration in a fully developed turbulent boundary layer with specific reference to the influence of particle inertial response to the underlying flow field. Statistical analysis of particle and fluid velocity fields has shown the crucial effect of inertia in determining particle sampling of specific flow regions. As a consequence of the preferential sampling, particles form clusters and accumulate in the near-wall region. We quantified the tendency of particles to form clusters by means of the Jacobian, $J(t)$, of the dispersed phase. Lagrangian statistics of $J(t)$ show that, within the time span covered by the simulations and in the range of particle relaxation times considered, the particle velocity field is more likely to be compressible and that inertial particles sample preferentially flow regions in which their local concentration is higher with respect to the initial conditions. An increase in particle inertia appears to enhance this trend.

The overall picture resulting from this statistical analysis shows the following features: (i) according to their dimension, particle sample the flow field selectively and exhibit a "turbulence" which also depends on their timescale; (ii) particles show a local turbophoresis which, in the present non-homogeneous turbulent channel flow, gives rise to a macroscale migration towards the wall; (iii) particle accumulation may be suitably quantified in a Lagrangian way by the behavior of

the Jacobian. Further investigation is required to establish the appropriate use of J to quantify compressibility when longer simulation times are considered.

References

Aris, R., 1989. Vectors, Tensors and the Basic Equations of Fluid Mechanics. Dover, New York.

Brooke, J.W., Kontomaris, K., Hanratty, T.J., McLaughlin, J.B., 1992. Turbulent deposition and trapping of aerosols at a wall. Phys. Fluids A 14, 825–834.

Caporaloni, M., Tampieri, F., Trombetti, F., Vittori, O., 1975. Transfer of particles in nonisotropic air turbulence. J. Atmos. Sci. 32, 565–568.

Chong, M.S., Perry, A., Cantwell, B.J., 1990. A general classification of three-dimensional flow fields. Phys. Fluids A 2, 765–777.

Crowe, C., Sommerfeld, M., Tsuji, Y., 1998. Multiphase Flows with Droplets and Particles. CRC Press, New York.

Eaton, J.K., Fessler, J.R., 1994. Preferential concentration of particles by turbulence. Int. J. Multiphase Flow 20, 169–209.

Elghobashi, S., Truesdell, G.C., 1992. Direct simulation of particle dispersion in a decaying isotropic turbulence. J. Fluid Mech. 242, 655–700.

Kim, J., Moin, P., Moser, R., 1987. Turbulence statistics in fully developed channel flow at low Reynolds number. J. Fluid Mech. 177, 133–166.

Lam, K., Banerjee, S., 1992. On the condition of streak formation in bounded flows. Phys. Fluids A 4, 306–320.

Lyons, S.L., Hanratty, T.J., McLaughlin, J.B., 1991. Large-scale computer simulation of fully developed turbulent channel flow with heat transfer. Int. J. Numer. Meth. Fluids 13, 999–1028.

Marchioli, C., Soldati, A., 2002. Mechanisms for particle transfer and segregation in turbulent boundary layer. J. Fluid Mech. 468, 283–315.

Marchioli, C., Giusti, A., Salvetti, M.V., Soldati, A., 2003. Direct numerical simulation of particle wall transfer and deposition in upward turbulent pipe flow. Int. J. Multiphase Flow 29, 1017–1038.

Maxey, M.R., Riley, J.K., 1983. Equation of motion for a small rigid sphere in a nonuniform flow. Phys. Fluids A 26, 883–889.

Maxey, M.R., 1987. The gravitational settling of aerosol particles in homogeneous turbulence and random flow fields. J. Fluid Mech. 174, 441–465.

Narayanan, C., Lakehal, D., Botto, L., Soldati, A., 2003. Mechanisms of particle deposition in a fully developed turbulent channel flow. Phys. Fluids A 15, 763–775.

Osiptsov, A.N., 1998. Modified Lagrangian method for calculating the particle concentration in dusty-gas flows with intersecting particle trajectories. In: Proceedings of the Third International Conference on Multiphase Flow (ICMF-98), Paper 236, Lyon, France.

Pope, S.B., 2000. Turbulent Flows. Cambridge University Press, Cambridge.

Portela, L.M., Cota, P., Oliemans, R.V.A., 2002. Numerical study of the near-wall behaviour of particles in turbulent pipe flows. Powder Technol. 125, 149–157.

Reeks, M.W., 1977. On the dispersion of small particles suspended in an isotropic turbulent fluid. J. Fluid Mech. 83, 529–546.

Reeks, M.W., 1983. The transport of discrete particles in inhomogeneous turbulence. J. Aerosol Sci. 310, 729–739.

Reeks, M.W., 1993. On the constitutive relations for dispersed particles in nonuniform flows 1. Dispersion in a simple shear flow. Phys. Fluids A 5, 750–761.

Rouson, D.W., Eaton, J.K., 2001. On the preferential concentration of solid particles in turbulent. J. Fluid Mech. 428, 149–169.

van Haarlem, B., Boersma, B.J., Nieuwstadt, F.T.M., 1998. Direct numerical simulation of particle deposition onto a free-slip and no-slip surface. Phys. Fluids A 10, 2608–2620.

Wang, L.P., Maxey, M.R., 1993. Settling velocity and concentration distribution of heavy particles in homogeneous isotropic turbulence. J. Fluid Mech. 256, 27–68.